JOURNAL OF VIROLOGY, Dec. 1995, p. 7851–7856 Vol. 69, No. 12
0022-538X/95/$04.00+0

Regulation of Coronavirus mRNA Transcription

GUIDO VAN MARLE, WILLEM LUYTJES, ROBBERT G. VAN DER MOST, TAHAR VAN DER STRAATEN, AND WILLY J. M. SPAAN*

Department of Virology, Institute of Medical Microbiology, Faculty of Medicine, Leiden University, 2300 AH Leiden, The Netherlands

Received 30 June 1995/Accepted 19 September 1995

Coronaviruses synthesize a nested set of six to eight subgenomic (sg) mRNAs in infected cells. These mRNAs are produced in different, but constant, molar ratios. It is unclear which factors control the different levels of sg mRNAs. To determine whether the intergenic sequence (IS) involved in sg mRNA synthesis could affect the transcription efficiencies of other ISs and in this way regulate transcription levels, we inserted multiple ISs at different positions into a mouse hepatitis virus defective interfering RNA. Quantitation of the sg RNAs produced by identical ISs in different sequence contexts led to the following conclusions: (i) transcription efficiency depends on the location of the IS in the defective interfering virus genome, (ii) downstream ISs have a negative effect on transcription levels from upstream ISs, and (iii) upstream ISs have little or no effect on downstream ISs. The observation that a downstream IS downregulates the amounts of sg RNA produced by an upstream IS explains why the smaller sg RNAs are, in general, produced in larger quantities than the larger sg RNAs. Our data are consistent with coronavirus transcription models in which ISs attenuate transcription. In these models, larger sg RNAs are synthesized in smaller amounts because they encounter more attenuating ISs during their synthesis.

During infection, coronaviruses produce a 3′-coterminal nested set of subgenomic (sg) mRNAs which are transcribed independently (6, 33). These sg mRNAs contain a common leader sequence derived from the 5′ end of the genome. For mouse hepatitis virus (MHV), this leader sequence is 72 nucleotides (nt) in length (28). The joining of the 5′ leader RNA to the mRNA is believed to be a discontinuous transcription process (11, 25). On the genome, the transcription units for the mRNAs are preceded by short, conserved sequence elements, referred to as intergenic sequences (ISs) (30). For MHV, every IS contains the sequence 5′ AAUCUAAAC 3′ or a closely related sequence (1, 9, 23). These IS elements are thought to function as promoters for sg mRNA synthesis (16, 30).

To explain the synthesis of leader-containing sg mRNAs, it has been proposed that short leader RNA species act as primers (10, 26). According to this so-called leader-primed transcription model, short leader RNAs are transcribed from the 3′ end of the antigenome, translocated to an IS on the negative-strand template, and then elongated to form leader-containing sg RNAs. In the original leader-primed transcription model, the template for transcription was a single, genome-length minus strand (12). However, the discovery of sg-size negative strands (5, 20, 24) has created questions on the nature of the template(s) for transcription. Recently, it has been demonstrated that the sg negative strands are transcriptionally active (20, 21). These results have led to several new transcription models.

Sethna et al. (22) speculated that first sg mRNAs are produced in the classic leader-primed fashion. These sg mRNAs are then used as templates for the synthesis of sg negative strands. Subsequently, the sg mRNAs are amplified from their negative-strand counterparts as replicons. However, to date, all attempts to obtain direct evidence for mRNA replication have failed. Transfecting synthetic mRNAs into coronavirus-infected cells did not result in replication of the sg RNA (2, 14, 16), but it could well be that transfected sg RNAs are not suitable templates for replication.

An alternative model has been proposed by Sawicki and Sawicki (20). They suggested that first a nested set of sg negative strands is synthesized and that these RNAs serve as templates for the synthesis of the corresponding mRNA and not vice versa. In principle, the discontinuous transcription step, in which the leader sequence is attached to the mRNA body sequence, could still take place, via leader priming on the sg negative strands or during negative-strand RNA synthesis.

A major question that remains to be answered is how the levels of sg mRNA are regulated. It has previously been postulated that the extent of base pairing between the leader and the IS on the negative strand would control transcription levels (24). However, we recently demonstrated that the extent of base pairing does not control mRNA abundance, nor is it regulated by the sequence of the IS itself (30).

Coronavirus mRNAs are, in general, synthesized in amounts that are inversely related to their size. It is possible that the size of the mRNA determines its abundance. However, it has been proposed that the generation of this apparent gradient of sg mRNA arises because larger RNA molecules are more prone to premature transcription termination and therefore produced in lesser quantities than smaller RNAs (9). This attenuation of transcription could occur during either of the two phases of transcription. RNA transcription initiation events on a downstream IS on the negative-strand template may cause the polymerase to pause, followed by premature termination of transcription, and so attenuate positive-strand synthesis (9). Alternatively, attenuation could occur during negative-strand synthesis (20) because of differential premature termination on the ISs. This latter idea is consistent with the model proposed by Sawicki and Sawicki. In this case, larger negative strands are produced in smaller quantities than the smaller strands because they have to be synthesized across more transcription-attenuating ISs on the positive-strand template. In this view, the levels of sg RNAs would be determined primarily by the amounts of sg negative strands.

To test the hypothesis that transcription attenuation is an

* Corresponding author. Phone: (31)-71-261652. Fax: (31)-71-263645. Electronic mail address: azruviro@rulcri.LeidenUniv.nl.

TABLE 1. Sequences and characteristics of oligonucleotides

Oligonucleotide	Sequence (5′→3′)	Polarity[a]	Position (nt) in MIDSal	Purpose
C066	CGCGCATAAT(C/G)TAAACAT	+		Cassette I
C067	CGCGATGTTTA(G/C)ATTATG	−		Cassette I
C082	AATTGTAAT(C/G)TAAAC	+		Cassette II
C081	AATTGTTTA(G/C)ATTAC	−		Cassette II
068	TTTTATGGATTTAGATGATG	+	4410–4430	Sequence analysis
C111	GGCTCCAACAGTTGGTGCCTTC	+	4784–4805	Sequence analysis
C015	ATTCATTCTCTGTCGA	−	5197–5212	Hybridization

[a] −, antisense; +, sense.

important factor controlling the levels of sg mRNAs, we inserted multiple wild-type (wt) and mutant (mut) mRNA3 ISs at different positions into an MHV defective interfering (DI) RNA vector. For this purpose, we have used a full-length cDNA clone of a naturally occurring DI RNA, pMIDI-C (29). Quantitation of the levels of sg DI RNAs produced by the different DI constructs led us to conclude that a functional downstream IS attenuates transcription from an upstream IS and not vice versa. Moreover, we found that transcription efficiency is also determined by the position of the promoter on the DI genome. The implications of our findings for the mechanism of transcription of coronaviruses are discussed.

MATERIALS AND METHODS

Cells and viruses. Mouse L cells and 17Cl1 cells were grown in Dulbecco's modified Eagle's medium containing 10% fetal calf serum. 17Cl1 cells were used for the production of high-titered virus stocks of MHV-A59 (19). All transfection and passaging experiments were performed with mouse L cells (27).

Recombinant DNA techniques. Standard recombinant DNA procedures were used (18). Restriction enzymes, T4 DNA ligase, and T4 polynucleotide kinase were obtained from Gibco BRL. The T7 sequencing kit of Pharmacia and [α-^{33}P]dATP of NEN-Dupont were used for DNA sequence analysis. All enzyme incubations and biochemical reactions were performed according to the instructions of the manufacturers.

Construction of the multiple promoter-containing DI constructs. Oligonucleotide cassettes containing a mixture of wt and mut mRNA3 ISs were obtained by mixing complementary oligonucleotides (Table 1) in equimolar amounts in a buffer containing 50 mM NaCl, 8 mM $MgCl_2$, 1 mM dithiothreitol, and 10 mM Tris-HCl (pH 7.5). The oligonucleotides were annealed by slowly decreasing the temperature from 95 to 4°C. The resulting double-stranded cassettes contained either *Mlu*I (cassette I) or *Eco*RI (cassette II) sticky ends. To prevent the formation of concatamers, a 1,000- to 2,000-fold molar excess of nonphosphorylated double-stranded oligonucleotides was used during ligation with phosphorylated vector DNA at 16°C. Cassettes I and II eliminated either the *Mlu*I (cassette I) or *Eco*RI (cassette II) site upon insertion. To select for plasmids containing oligonucleotide cassette insertions, the ligation mixtures were digested with either *Mlu*I or *Eco*RI prior to transformation. Since cassettes I and II contain mutations, the desired inserts were selected by sequencing with oligonucleotides 068 and C111 (Table 1).

To obtain DI constructs containing combinations of wt and mut mRNA3 ISs, oligocassette I, containing a mixture of wt and mut ISs, was inserted in the *Mlu*I site at position 4435 of pDIRA/wt and pDIRA1 (30). pDIRA/wt and pDIRA1 are pMIDSal derivatives containing a wt and mut mRNA3 promoter in the *Sal*I site at position 5196 (Fig. 1; note that positions in the figure and in the text refer to pMIDSal). The resulting constructs were used to insert a third mRNA3 IS (wt and mut) at the *Eco*RI site at position 4835. First, the *Pst*I fragment (positions 1145 to 2508), containing an additional *Eco*RI site, was removed. Oligocassette II was inserted into the unique *Eco*RI site of the resulting plasmid. After insertion of the oligonucleotide cassette, the *Pst*I fragment was inserted, resulting in DI constructs containing all possible combinations of three functional and nonfunctional mRNA3 ISs (Fig. 1).

In vitro transcription and transfection. Plasmid DNA was linearized by using restriction endonuclease *Nhe*I. In vitro transcripts were generated with T7 RNA polymerase and transfected into mouse L cells with lipofectin (Bethesda Research Laboratories). In vitro transcription and RNA transfection were performed as described previously (29). MHV-A59 was used as a helper virus in all transfections.

Isolation and analysis of viral RNAs. Intracellular RNAs were isolated as described by Spaan et al. (27). RNAs were separated on 1% agarose gels containing 2.2 M formaldehyde and MOPS buffer (10 mM MOPS [morpholinepropanesulfonic acid {sodium salt}] [pH 7], 5 mM sodium acetate, 1 mM EDTA). Subsequently, the RNAs were transferred to Hybond N$^+$ membranes (Amersham) by electroblotting in MOPS buffer and then were hybridized with 100 ng of 5′-end-labelled oligonucleotide C015 (Table 1) (17). Oligonucleotides were labelled with [γ-^{32}P]ATP (NEN-Dupont) and T4 polynucleotide kinase. Quantitation of the radioactive blots was performed with a Betascope (Betagene). Statistics, including mean ± standard deviation and *F* and Student *t* tests, were performed by using Microsoft Excel 5.0 (Microsoft Corporation).

Oligonucleotides. An Applied Biosystems 391 PCR MATE oligonucleotide synthesizer was used for the synthesis of oligonucleotides.

RESULTS

Construction of DI RNAs with multiple ISs. To investigate how ISs influence each other, the IS element of mRNA3 was introduced at three different positions in the genome of the synthetic DI RNA MIDSal (30) (Fig. 1). This approach also allowed us to study the effect of the location of an IS on its transcription efficiency. The plasmid from which MIDSal RNA is transcribed, pMIDSal, is a derivative of pMIDI-C in which a *Sal*I site was introduced directly downstream of the DI open reading frame (ORF) (30). pMIDI-C is a full-length cDNA clone of a naturally occurring MHV-A59 DI RNA (31). We inserted wt mRNA3 ISs (5′ UAAUCUAAAC 3′); as a control, we inserted mut mRNA3 ISs (5′ UAAUGUAAAC 3′), which are transcriptionally inactive because of the C-to-G substitution (30). The ISs were inserted as double-strand cassettes in the *Mlu*I, *Eco*RI, and *Sal*I sites of pMIDSal. These positions will be referred to as A, B, and C, respectively, in the DI RNA (Fig. 1). Since the ORF which is present in the MHV-A59 DI RNA is required for efficient propagation of the DI (4, 32), the IS insertions at positions A and B were made in frame.

We constructed a panel of recombinant DI RNAs containing all possible combinations of three wt and mut mRNA3 ISs (Fig. 1). The DI constructs are named after the positions of the ISs in the DI genome. The wt ISs are indicated by capital letters, and mut ISs are indicated by lowercase letters. For instance, DI construct Abc contains a functional wt mRNA3 IS at position A and mutant mRNA3 ISs at positions B and C of the DI genome. The resulting DI constructs were expected to produce one, two, three, or no sg DI RNAs. The sg DI RNAs produced by the ISs at positions A, B, and C should have sizes of 1.2, 0.75, and 0.4 kb, respectively. These sg RNAs will be referred to hereafter as sg RNAs A, B, and C, and their corresponding ISs will be referred to hereafter as ISs A, B, and C. Throughout this study, transcription efficiency is defined as the amount of sg DI RNA relative to the genomic DI RNA (16, 30), as determined by beta-scanning of Northern (RNA) blots.

Transcription efficiencies of DI-borne ISs A, B, and C. In vitro-transcribed RNAs of the DI constructs were transfected into MHV-A59-infected L cells. After 16 h, the progeny virus (P0) was harvested and used to inoculate fresh L cells. The resulting P1 virus stock was used to inoculate fresh L cells, from which RNA was isolated, 7 to 8 h postinfection (P2 RNA). The P2 RNA preparations were separated on formal-

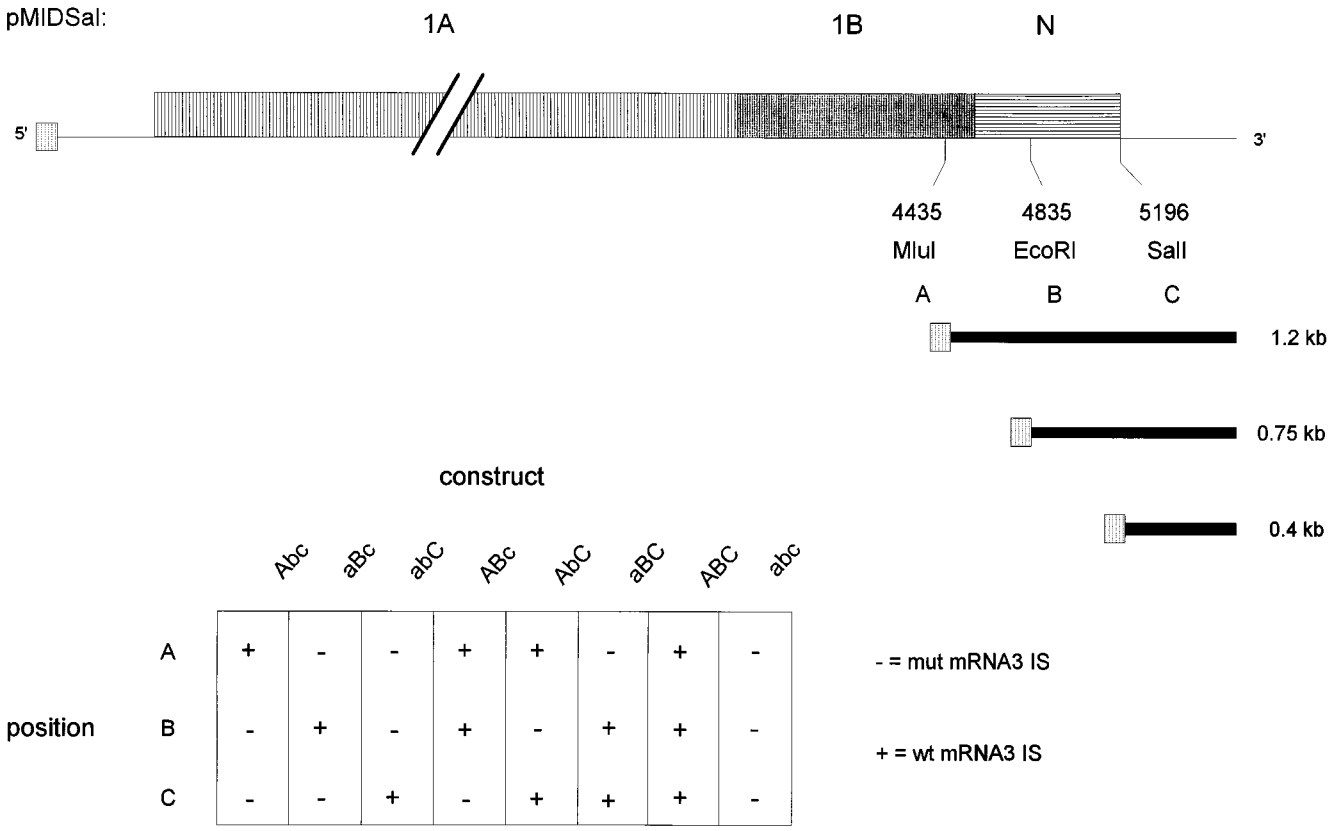

FIG. 1. Schematic representation of DI constructs. The pMIDSal construct is outlined at the top. The boxes indicate the regions (polymerase ORF 1A [1A], polymerase ORF 1B [1B], and nucleocapsid gene [N]) derived from the MHV-A59 genome which constitute the DI. The small box at the 5′ end depicts the leader. The restriction enzyme recognition sites in which ISs were inserted are indicated. The numbers represent their distances (in nucleotides) from the start of the synthetic RNA. The three insertion sites are referred to as positions A, B, and C in the DI. The black bars indicate the relative sizes of the sg RNAs produced from the ISs at positions A, B, and C on the DI. The complete panel of DI constructs, containing each possible combination of three mutant and wt ISs, is shown at the bottom of the figure.

dehyde-agarose gels, and viral RNAs were analyzed by Northern blotting. We specifically chose to use Northern blots instead of dried gels for hybridization, since a fraction of the smaller subgenomic DI RNAs might be lost during the drying process, resulting in an underrepresentation of these RNA molecules (data not shown). For probing the Northern blots, we used radiolabelled oligonucleotide C015 (Table 1). This probe specifically binds to the DI constructs and their sg DI RNAs. It does not detect DI RNAs that have lost the inserted ISs by recombination with the viral genome (31). However, the probe has some residual affinity for MHV RNAs 1 to 7 and cross-hybridizes with the 18S and 28S rRNAs which are visible as extra bands on the blots.

The Northern blot analysis of the intracellular RNAs showed that all DIs replicated efficiently and produced sg DI RNAs of the expected lengths (Fig. 2). The transcription efficiencies of the ISs at positions A, B, and C in the several DI constructs were determined in seven independent experiments (Table 2).

Our data clearly demonstrate that the constructs Abc, aBc, and abC produced different amounts of sg DI RNA. The IS at position B in construct aBc gave rise to the largest amount of sg RNA, approximately twice as much as the IS at position C in construct abC. The IS at position A in construct Abc produced the smallest amounts of sg RNA. Accordingly, in construct ABC, sg RNA B was the most abundant and sg RNA A was the least abundant. Also in constructs ABc, AbC, and aBC, the 1.2-kb sg RNA A was the least abundant and the 0.75-kb sg RNA B was the most abundant sg DI RNA species. Thus, insertion of multiple functional ISs into the DI constructs yielded the same pattern of sg RNA abundances as the DIs containing a single functional IS. These results strongly suggest that the position of an IS on the genome can have a major effect on the amounts of sg RNA that are produced. It is also

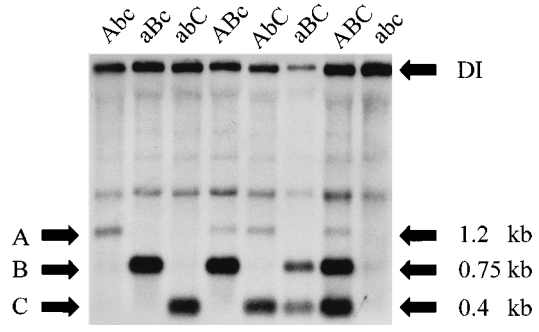

FIG. 2. Northern blot analysis of intracellular RNAs. L cells were infected with MHV-A59 and transfected with the synthetic DI RNAs, and progeny virus was passaged twice. P2 RNA was isolated and separated on formaldehyde-agarose gels, blotted onto nylon membranes, and hybridized with 5′-end-labelled oligonucleotide C015. The positions of the DI RNAs and sg DI RNAs (referred to as A, B, and C) are indicated by arrows.

TABLE 2. Transfection efficiencies

Construct	Transcription efficiency[a]		
	IS A	IS B	IS C
Abc	27 ± 13	–	–
aBc	–	227 ± 94	–
abC	–	–	91 ± 22
ABc	8 ± 7	254 ± 36	–
AbC	13 ± 10	–	103 ± 33
aBC	–	164 ± 22	109 ± 58
ABC	7 ± 5	133 ± 18	107 ± 42
abc	–	–	–

[a] The ratio (and standard deviation) between the amount of sg DI RNA and genomic DI RNA, determined by beta-scanning of Northern blots in seven independent experiments. –, no sg RNA detected.

clear from our data that the smallest sg RNA does not necessarily have to be the most abundant. In other words, the abundance of an sg RNA does not seem to be a function of its size. We also observed that the presence of one or more functional ISs did not have a major impact on the accumulation of the parental genomic DI RNA. In all experiments, the DIs accumulated to similar levels whether they were producing sg RNA or not (data not shown) (Fig. 2).

Transcription efficiencies are influenced by adjacent ISs. A comparison of the transcription efficiency of a given IS in the presence or absence of other functional ISs (Table 2) suggested that the presence of additional functional ISs was influencing transcription efficiency. To investigate this in more detail, we performed a statistical analysis on the data shown in Table 2 by using a cutoff value of $P = 0.05$.

For IS A, an F test showed significant differences ($P = 0.04$) in the amounts of sg RNA produced in the presence or absence of functional ISs at positions B and C. In a subsequent Student t test, we compared construct Abc with the other constructs. This test showed that the amounts of sg RNA A decreased significantly in the presence of a functional IS at position B (construct ABc, $P = 0.006$), C (construct AbC, $P = 0.04$), or B and C (construct ABC, $P < 0.001$). Similarly, for the IS at position B, the F test showed significant differences ($P = 0.038$) in the amounts of sg RNA produced in the presence or absence of other functional ISs. The Student t test showed that the transcription efficiency of IS B in construct aBc differed significantly from the transcription efficiency of this IS in the presence of functional ISs at position C (construct aBC, $P = 0.026$) or A and C (construct ABC, $P = 0.048$). However, in the case of construct ABc, the functional IS at position A, upstream of B, had no significant effect ($P = 0.501$) on the amounts of sg RNA B. Thus, it appears that functional downstream ISs affect the transcription efficiency of upstream ISs but not vice versa. In accordance with this notion, the F test showed no significant difference ($P = 0.7$) in the levels of sg RNA produced by IS C in the presence or absence of functional upstream ISs, i.e., at positions A and B.

In conclusion, our data indicate that the transcriptional efficiency of an IS is downregulated by functional downstream ISs, while functional upstream ISs do not influence downstream ISs. We observed this inhibitory effect over distances ranging from 361 to 400 (in constructs ABC, ABc, and aBC) to 761 (in construct AbC) nt.

DISCUSSION

Until now, most studies on coronavirus transcription using DI RNAs have focused on transcription from a single IS. Coronaviruses produce more than one mRNA, and it is possible that the transcriptional activities of the ISs influence each other and that this plays a role in controlling coronavirus sg RNA levels. To address this issue, we inserted wt and mut mRNA3 ISs at multiple positions (denoted A, B, and C) into our DI RNA vector.

The position of an IS affects transcriptional efficiency. Analysis of the DI constructs containing a single functional IS revealed a clear difference in the amounts of sg RNA produced by the mRNA3 ISs at positions A, B, and C of the DI genome. The IS at position B in construct aBc produced the largest amounts of sg RNA, while the IS at position A in construct Abc produced the smallest amounts. The pattern of sg RNA accumulation in the DIs containing multiple functional ISs was similar to that of the constructs containing one functional IS, i.e., the product of the IS B was the most abundant and that of the IS A was the least abundant. These data suggest that the position of the IS on the DI genome strongly affects the amounts of sg RNA it produces. This observation is in accordance with earlier data showing that the amounts of sg RNA that are generated by an IS can depend on the flanking sequences, which are not specific (8, 15). The influence of the flanking sequences could stem from the overall RNA secondary structure. Recently, Zhang and Lai found a correlation between the amounts of sg RNA produced by wt and mut MHV mRNA2 ISs and the affinities of cellular proteins for these ISs (34). From our study, it is clear that the differences in transcription efficiencies cannot be explained by differences in the affinities of these proteins for the IS because we used the same mRNA3 IS at positions A, B, and C. What we cannot exclude is that the observed differences in sg RNA abundances are caused by differences in RNA stabilities. This is a possibility that we are currently testing.

For MHV, there is an inverse correlation between size and abundance of sg mRNA. In MHV-infected cells, the smallest RNA is the most abundant. This correlation is not observed for the coronaviruses transmissible gastroenteritis virus (TGEV) (22) and feline infectious peritonitis virus (FIPV) (3). In both these viruses, the smallest mRNA accumulates to lower levels than that of the next larger mRNA. Interestingly, the pattern of sg RNA accumulation observed for construct ABC bears resemblance to that of TGEV and FIPV, i.e., the smallest of the three sg RNAs produced by construct ABC was not the most abundant. Since a direct correlation between size and sg RNA abundance was not seen for any of our constructs, we conclude that the size of the RNA does not exclusively determine its accumulation.

We observed that the production of sg RNAs from the DI construct did not have a major effect on its accumulation. The DI RNAs producing one or more sg DI RNAs accumulated to levels similar to that of the DI RNA producing no sg RNAs. This would suggest that transcription and replication do not influence each other. These data are in conflict with the observations of Jeong and Makino (7) and Lin et al. (13). They reported that sg DI RNA synthesis from MHV-JHM-derived DI constructs inhibited the replication of the DI genome. What causes these different observations is unclear.

Transcription efficiency is influenced by adjacent ISs. The aim of our study was to investigate factors that rule coronavirus mRNA synthesis. One of the factors we investigated was how the transcription efficiency of a given IS is influenced in *cis* by the presence of other ISs. Determining the transcription efficiencies of the functional ISs in our DI constructs showed a significant inhibition by the presence of functional ISs downstream. However, there was no significant effect of functional ISs on downstream ISs. We observed that functional down-

stream ISs could have inhibitory effects over distances of 361 to 400 nt (constructs ABC, ABc, and aBC) and 761 nt (construct AbC).

In an earlier study of MHV transcription, Joo and Makino (8) have investigated the transcription efficiencies of two adjacent ISs. The distances between these two ISs varied from 23 to 124 nt. They concluded that there was a dramatic inhibition of the transcription efficiency of an upstream IS by the downstream IS when the ISs were 23 nt apart. The extent of inhibition decreased as the distance between the ISs increased. ISs that were 124 nt apart produced almost equal amounts of sg RNA. Joo and Makino (8) explained this strong inhibition of upstream ISs by downstream ISs by steric hindrance. Binding of transcription factors or the transcription complex on the downstream IS could limit the accessibility of the upstream IS if they are close together (i.e., 23 nt). In our study, the distances between the ISs ranged from 361 to 761 nt, therefore it is unlikely that the inhibition of an upstream IS by a downstream IS is caused by steric hindrance. Neither can this inhibitory effect be caused by competition for the polymerase, since this would result in inhibition of transcription of all ISs, which is not what we observed. In fact, the observation that downstream ISs attenuate upstream ISs and not vice versa is consistent with two models for coronavirus transcription (9, 20) (Fig. 3).

Konings et al. (9) proposed, on the basis of the available data at that time, that attenuation occurring during positive-strand synthesis determines mRNA levels. Transcription starts on an IS on the negative-strand genomic template by leader priming. When the polymerase encounters a functional downstream IS during positive-strand synthesis, it pauses because of initiation of transcription on the downstream IS. This may result in termination of transcription by the polymerase. The more the polymerase is forced to pause, the more chance it has to terminate and consequently, the less RNA it will make. Thus, the initiation events on downstream ISs are the attenuating factors for transcription. In a more recent model proposed by Sawicki and Sawicki (20), attenuation of transcription occurs during negative-strand synthesis. In this model, the ISs on the positive-strand template function as transcription attenuators or even differential terminators for negative-strand synthesis. This would result in the formation of a nested set of sg negative strands. A portion of the polymerases detaches from the positive-strand template when it reaches an IS sequence to form an sg negative strand. Thus, the synthesis of a larger sg negative strand, i.e., the product of the upstream IS, is attenuated by the presence of a downstream IS because only a percentage of the polymerase complexes reach the upstream IS. The anti-leader on the sg minus strand is transcribed either after a template jump to the 5′ end of the genome or after hybridization of leader fragments to the nascent minus-strand IS.

In either model it is unclear what physically causes the polymerase to pause during positive-strand synthesis or to terminate during minus-strand synthesis. Proteins bound to the IS on the negative or positive strand may play a role. These proteins could be of viral origin or host proteins. The recent finding that host proteins bind to the wt ISs and not to mutant ISs (34) is consistent with this hypothesis. However, the nature and function of these proteins remain to be determined.

Although our data indicate that attenuation of transcription by downstream ISs does occur, we cannot discriminate between attenuation during negative- or positive-strand synthesis. A recent study on coronavirus transcription done by Schaad and Baric (21) strongly suggests that sg negative strands are functional and play an important role in transcription. This observation would favor attenuation according to the transcription model proposed by Sawicki and Sawicki (20).

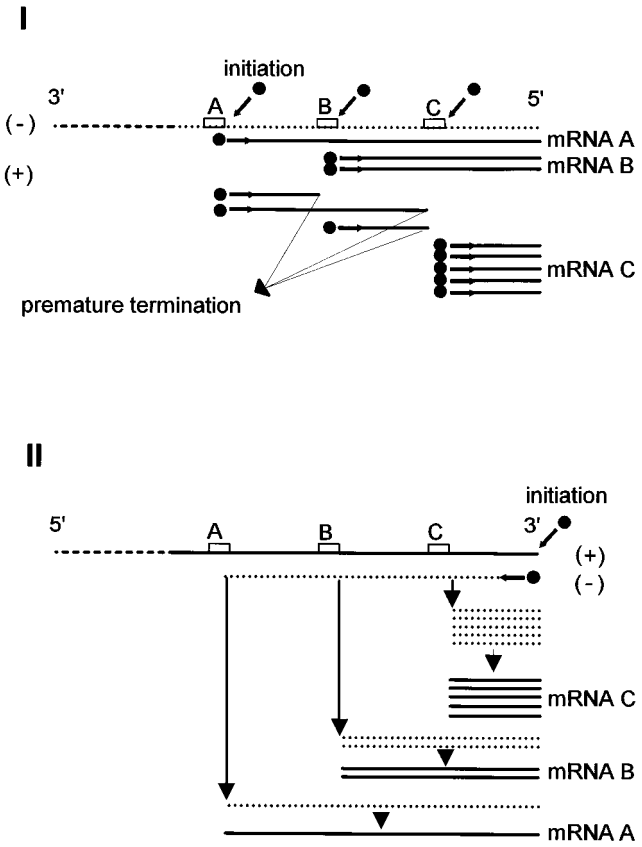

FIG. 3. The models for transcription attenuation as proposed by Konings et al. (9) (I) and Sawicki and Sawicki (20) (II). The ISs (A, B, and C) on the positive- and negative-strand template are indicated with boxes. Plus- and minus-strand RNAs are represented by solid and dotted lines, respectively, and by plus and minus signs within parentheses. The polymerase complex is depicted as a black circle; the associated arrows symbolize initiation events. During plus-strand synthesis (I), transcription pauses on a downstream IS because of initiation events on that IS. Subsequently, transcription is either resumed, yielding mRNA A or B, or terminates prematurely. The amount of a particular sg RNA synthesized depends on the frequency of premature termination which is a function of the duration of the pausing and on the number of ISs that have to be passed. The smallest mRNA should be produced more efficiently because it is not hampered in its synthesis by downstream ISs. During minus-strand synthesis (II), a portion of the polymerases detaches from the positive-strand template after reaching an IS and releases sg minus strands while the remaining polymerases continue synthesis. Larger sg minus strands will be produced less efficiently than smaller ones because they have to be synthesized across more ISs where ever-smaller portions of the polymerases remain. The amount of sg minus strands produced will determine the levels of sg mRNAs.

In conclusion, we have demonstrated that two different principles can govern the synthesis of sg RNAs in coronaviruses. The DI constructs containing multiple ISs demonstrated that attenuation of the transcription levels of sg RNAs by downstream ISs occurs, which would lead to a gradient of sg RNAs in which the smaller sg RNAs are synthesized at higher levels. From the data obtained with the DI constructs containing a single functional IS, we show that its position on the genome can determine the level of sg RNA produced, in a nongradient fashion. Both principles apparently play a role in coronavirus transcription simultaneously. This explains the sg RNA patterns for constructs ABC and aBC and also those of coronaviruses TGEV and FIPV. The factors involved in attenuation

(e.g., protein binding) and the position effect (e.g., RNA secondary structure and stability) are currently under study.

ACKNOWLEDGMENTS

We thank Stanley and Dorothea Sawicki for stimulating discussions and Heleen Gerritsma for technical assistance.

G.V.M. was supported by grant 331-020 from the Dutch Foundation for Chemical Research (SON). W.L. is a fellow of the Royal Dutch Academy for Sciences (KNAW).

REFERENCES

1. **Budzilowicz, C. J., S. P. Wilczynski, and S. R. Weiss.** 1985. Three intergenic regions of coronavirus mouse hepatitis virus strain A59 genome RNA contain a common nucleotide sequence that is homologous to the 3′ end of the viral mRNA leader sequence. J. Virol. **53:**834–840.
2. **Chang, R.-Y., M. A. Hofmann, P. B. Sethna, and D. A. Brian.** 1994. A *cis*-acting function for the coronavirus leader in defective interfering RNA replication. J. Virol. **68:**8223–8231.
3. **de Groot, R. J., R. J. ter Haar, M. C. Horzinek, and B. A. M. van der Zeijst.** 1987. Intracellular RNAs of the feline infectious peritonitis coronavirus strain 79–1146. J. Gen. Virol. **68:**995–1002.
4. **de Groot, R. J., R. G. van der Most, and W. J. M. Spaan.** 1992. The fitness of defective interfering murine coronavirus DI-a and its derivatives is decreased by nonsense and frameshift mutations. J. Virol. **66:**5898–5905.
5. **Hofmann, M. A., P. B. Sethna, and D. A. Brian.** 1990. Bovine coronavirus mRNA replication continues throughout persistent infection in cell culture. J. Virol. **64:**4108–4114.
6. **Jacobs, L., W. J. M. Spaan, M. C. Horzinek, and B. A. M. van der Zeijst.** 1981. Synthesis of subgenomic mRNAs of mouse hepatitis virus is initiated independently: evidence from UV transcription mapping. J. Virol. **39:**401–406.
7. **Jeong, Y. S., and S. Makino.** 1992. Mechanism of coronavirus transcription: duration of primary transcription initiation activity and effects of subgenomic RNA transcription on RNA replication. J. Virol. **66:**3339–3346.
8. **Joo, M., and S. Makino.** 1995. The effect of two closely inserted transcription consensus sequences on coronavirus transcription. J. Virol. **69:**272–280.
9. **Konings, D. A. M., P. J. Bredenbeek, J. F. H. Noten, P. Hogeweg, and W. J. M. Spaan.** 1988. Differential premature termination of transcription as a proposed mechanism for the regulation of coronavirus gene expression. Nucleic Acids Res. **16:**10849–10860.
10. **Lai, M. M., R. S. Baric, P. R. Brayton, and S. A. Stohlman.** 1984. Characterization of leader RNA sequences on the virion and mRNAs of mouse hepatitis virus, a cytoplasmic RNA virus. Proc. Natl. Acad. Sci. USA **81:**3626–3630.
11. **Lai, M. M. C.** 1990. Coronavirus—organization, replication and expression of genome. Annu. Rev. Microbiol. **44:**303–333.
12. **Lai, M. M. C., C. D. Patton, and S. A. Stohlman.** 1982. Replication of mouse hepatitis virus: negative-stranded RNA and replicative form RNA are of genome length. J. Virol. **44:**487–492.
13. **Lin, Y.-J., C.-L. Liao, and M. M. C. Lai.** 1994. Identification of the *cis*-acting signal for the minus-strand RNA synthesis of a murine coronavirus: implications for the role of minus-strand RNA in RNA replication and transcription. J. Virol. **68:**8131–8140.
14. **Luytjes, W., H. Gerritsma, and W. J. M. Spaan.** Unpublished results.
15. **Makino, S., and M. Joo.** 1993. Effect of intergenic consensus sequence flanking sequences on coronavirus transcription. J. Virol. **67:**3304–3311.
16. **Makino, S., M. Joo, and J. K. Makino.** 1991. A system for study of coronavirus mRNA synthesis: a regulated, expressed subgenomic defective interfering RNA results from intergenic site insertion. J. Virol. **65:**6031–6041.
17. **Meinkoth, J., and G. Wahl.** 1984. Hybridization of nucleic acids immobilized on solid supports. Anal. Biochem. **138:**267–284.
18. **Sambrook, J., E. F. Fritsch, and T. Maniatis.** 1989. Molecular cloning: a laboratory manual. Cold Spring Harbor Laboratory Press, Cold Spring Harbor, N.Y.
19. **Sawicki, S. G., and D. L. Sawicki.** 1986. Coronavirus minus-strand RNA synthesis and effect of cycloheximide on coronavirus RNA synthesis. J. Virol. **57:**328–334.
20. **Sawicki, S. G., and D. L. Sawicki.** 1990. Coronavirus transcription: subgenomic mouse hepatitis virus replicative intermediates function in RNA synthesis. J. Virol. **64:**1050–1056.
21. **Schaad, M. C., and R. S. Baric.** 1994. Genetics of mouse hepatitis virus transcription: evidence that subgenomic negative strands are functional templates. J. Virol. **68:**8169–8179.
22. **Sethna, P. B., S. L. Hung, and D. A. Brian.** 1989. Coronavirus subgenomic minus-strand RNAs and the potential for mRNA replicons. Proc. Natl. Acad. Sci. USA **86:**5626–5630.
23. **Shieh, C.-K., H. J. Lee, K. Yokomori, N. La Monica, S. Makino, and M. M. C. Lai.** 1989. Identification of a new transcriptional initiation site and the corresponding functional gene 2b in the murine coronavirus RNA genome. J. Virol. **63:**3729–3736.
24. **Shieh, C.-K., L. H. Soe, S. Makino, M. F. Chang, S. A. Stohlman, and M. M. C. Lai.** 1987. The 5′-end sequence of the murine coronavirus genome: implications for multiple fusion sites in leader-primed transcription. Virology **156:**321–330.
25. **Spaan, W., D. Cavanagh, and M. C. Horzinek.** 1988. Coronaviruses: structure and genome expression. J. Gen. Virol. **69:**2939–2952.
26. **Spaan, W., H. Delius, M. Skinner, J. Armstrong, P. Rottier, S. Smeekens, B. A. M. van der Zeijst, and S. G. Siddell.** 1983. Coronavirus mRNA synthesis involves fusion of non-contiguous sequences. EMBO J. **2:**1839–1844.
27. **Spaan, W. J. M., P. J. M. Rottier, M. C. Horzinek, and B. A. M. van der Zeijst.** 1981. Isolation and identification of virus-specific mRNAs in cells infected with mouse hepatitis virus (MHV-A59). Virology **108:**424–434.
28. **Spaan, W. J. M., P. J. M. Rottier, M. C. Horzinek, and B. A. M. van der Zeijst.** 1982. Sequence relationships between the genome and the intracellular RNA species 1, 3, 6, and 7 of mouse hepatitis virus strain A59. J. Virol. **42:**432–439.
29. **van der Most, R. G., P. J. Bredenbeek, and W. J. M. Spaan.** 1991. A domain at the 3′ end of the polymerase gene is essential for encapsidation of coronavirus defective interfering RNAs. J. Virol. **65:**3219–3226.
30. **van der Most, R. G., R. J. de Groot, and W. J. M. Spaan.** 1994. Subgenomic RNA synthesis directed by a synthetic defective interfering RNA of mouse hepatitis virus: a study of coronavirus transcription initiation. J. Virol. **68:**3656–3666.
31. **van der Most, R. G., L. Heijnen, W. J. M. Spaan, and R. J. de Groot.** 1992. Homologous RNA recombination allows efficient introduction of site-specific mutations into the genome of coronavirus MHV-A59 via synthetic co-replicating RNAs. Nucleic Acids Res. **20:**3375–3381.
32. **van der Most, R. G., W. Luytjes, S. A. Rutjes, and W. J. M. Spaan.** 1995. Translation but not the encoded sequence is essential for the efficient propagation of the defective interfering RNAs of the coronavirus mouse hepatitis virus. J. Virol. **69:**3744–3751.
33. **Yokomori, K., L. R. Banner, and M. M. C. Lai.** 1992. Coronavirus mRNA transcription: UV light transcriptional mapping studies suggest an early requirement for a genomic-length template. J. Virol. **66:**4671–4678.
34. **Zhang, X., and M. M. C. Lai.** 1995. Interactions between the cytoplasmic proteins and the intergenic (promoter) sequence of mouse hepatitis virus RNA: correlation with the amounts of subgenomic mRNA transcribed. J. Virol. **69:**1637–1644.